Endogenous Roles of NT5C2 Identified with Genetic Screening and Treatment Implications

Margarita Bogdanova-Shapkina

Oceanside High School

ABSTRACT

Aberrant over-expression of *NT5C2* has been linked to chemoresistance in relapsed acute lymphoblastic leukemia (ALL). Multiple gain-of-function *NT5C2* mutations have been identified that account for post-relapse chemoresistance in ALL patients. Preliminary data has shown that mutant NT5C2-containing ALL cells have demonstrated increased sensitivity to treatment with mizoribine, and that knockout and knockdown of NT5C2 has little effect on cell homeostasis and growth. In addition, NT5C2 splicing variants have been associated with hereditary spastic paraplegia. These indicate that there may be unknown compensatory mechanisms and/or endogenous roles of NT5C2. The purpose of the study was threefold: first, to identify the extent, if any, of the effects of NT5C2 KO on the cell (NT5C2 CRISPR KO and rescue and MTT/growth curve analysis of the effect on cellular population, and comparison of RNA sequencing between the variants to identify compensatory mechanisms); second, to identify any other genes that interfere with NT5C2's role in the purine biosynthesis pathway (investigated through whole genome mizoribine CRISPR screening); and third, to identify pathways directly affected by treatment-like pharmaceutical inhibition of NT5C2 through whole-genome CRISPR screening with HTP-2, an early-stage NT5C2 inhibitor. While the RNA sequencing and HTP-2 screen failed to yield results, mizoribine screening identified several pathways in which NT5C2 may be involved, whole growth curve comparison confirms the absence of any inherent cytotoxicity to NT5C2 inhibition or knockout. These results offer several potential new avenues besides direct NT5C2 inhibition for combating chemoresistance in ALL, and confirm NT5C2 as a viable treatment option where feasible.

INTRODUCTION

Acute Lymphoblastic Leukemia (ALL), the most common cancer found in pediatric patients, is an aggressive hematological malignancy characterized by infiltration of the bone marrow by anomalous immature lymphocytes/lymphoblasts (Belver and Ferrando, 2016). 20% of pediatric and over 50% of adult ALL patients experience disease relapse despite intensive chemotherapy

(Hunger and Mullighan, 2015). Relapsed ALL has demonstrated a high degree of resistance to chemotherapy drugs, primarily purine analog 6-MP, during the course of renewed treatment (Bahojwani et al, 2015). Activation mutations in *NT5C2*, the gene encoding cytosolic purine 5′-nucleotidase, have been identified as a driver of chemotherapy resistance in T-ALL as NT5C2's aberrantly increased purine nucleotidase activity inactivates 6-MP (Tzoneva et al, 2013), which is a purine analog, through digestion thereof (Bhatia et al, 2014). These activating mutations are sorted into three classes based on the conformational changes they cause: Class I mutations lock the activating A-helix that supports the structure of the active site in the inter-monomeric space, Class II mutations disrupt the "arm" residues of NT5C2, which act as switch-off mechanism by denaturing the A-helix, and Class III mutations add residues such that the A-helix can be formed without allosteric activation, meaning NT5C2 can be active without ATP (Dieck et al, 2018b).

Mutant NT5C2 chemoresistant ALL cells have been found exhibit significantly increased sensitivity to mizoribine, an IMPDH inhibitor, possibly due to radical depletion of the intracellular purine supply due to the combination of increased export by NT5C2 and suppressed production by mizoribine. This makes mizoribine a potential anti-leukemic drug and a compound known to relevantly interact with NT5C2 (Tzoneva et al, 2013). Also, NT5C2 mutations have been implicated in spastic paraplegia, suggesting that its full endogenous role and pathway participation is not limited to purine biosynthesis (Elsaid, 2017).

The full range of the intracellular roles of NT5C2, and the effect of its inhibition on cellular function and cell viability in general and in ALL, are currently unexplored yet remain a major

necessity in determining potential side effects during patient treatment as well as alternative routes towards eliminating chemoresistance in treatment.

METHODS

CRISPR Knockout of NT5C2

To determine what effect NT5C2 inhibition would have on cell viability and behavior, in anticipation of NT5C2 inhibitory therapies for relapsed ALL, a full CRISPR/Cas9-mediated knockout of NT5C2 in various ALL cell lines was performed. Three single guide gRNAs (respectively cleaving Exon 3, Exon 8, and Exon 13) were designed for *Mus musculus* using Benchling software. During synthesis, these gRNAs were attached to the pEGFP gene that confers green fluorescence by coding for GFP. The gRNA complexes were then each infected into CUTLL1 cells in a manner identical to the protocol used in the BioID infection/transfection stage into a 96-well plate, with 5 million cells and 150 μg genetic material per well. A second empty vector (EV) complex containing just pEGFP was also infected into CUTLL1 cells following the same protocol. After a 12-hour incubation at 37℃, Cas9 was added to all cells, which were then incubated for 96 hours. To confirm the efficacy of the designed gRNAs and the success of the CRISPR knockout of NT5C2, a T7 endonuclease assay was performed on a 50μL/100ng DNA sample from each group of cells. T7 endonuclease recognizes and digests non-perfectly matched DNA, allowing it to identify CRISPR/Cas9 activity as it results in non-homologous end joining at the DNA cleavage site. The 3 gRNA samples, the empty vector sample, and nuclease-free water, which acted as the non-template control, were PCR amplified using primers custom designed using Benchling and thermocycling in accordance with the standard T7 Endonuclease Assay protocol available through New England Biolabs. T7 Endonuclease I was then added to 50% of the amplified samples, allowing for a comparison of T7+ and T7- groups to confirm T7 Endonuclease I activity, followed by a PCR annealing reaction that resulted in DNA cleavage in the T7+, where CRISPR-caused fragmentation was present. Gel electrophoresis was then used to compare CRISPR activity between the different gRNAs, a decreased intensity of an NT5C2 band in a gRNA sample as compared to an EV

sample due to T7 digestion of fragmented DNA. The gRNA cleaving Exon 8 was found to be ineffective at this stage, and experimentation proceeded with the gRNAs cleaving Excons 3 and 13, hereafter referred to as "gRNA1" and "gRNA3," respectively.

Sorting and Suspension of NT5C2 KO Cells

The CUTLL1 cells successfully infected with the gRNA1, gRNA3, and EV complexes were selected from their initial group through fluorescence activated cell sorting (FACS), gating for the green fluorescence associated with the infected complexes, as well as size and shape ratios to filter live cells (BSC-A/FSC-A, FSC-H/FSC-A). Two negative control groups, including WT non-infected CUTLL1 cells, and WT *M. musculus* liver cells unrelated to ALL, also underwent FACS to confirm the validity of the procedure. After a 24-hour incubation period allowing sorted cells from the three groups to regain homeostatic stability, a manual 1:200 dilution with DMEM was performed such that one cell was was placed in each well of a 96-well plate. On a constant rolling basis, whenever noticeable cell growth was observed visually through increased well opacity, fluorescence spectroscopy was performed and wells with sufficient cell growth (abs > 0.5) were transferred to a 24-well plate to decrease confluence. Then, wells were observed through a microscope and those wells lacking a distinct cell colony originating from the single-cell suspension, containing foreign outgrowth or contamination, containing colonies from more than one initially suspended cell, or otherwise not properly originating from a single-cell suspension in a manner preserving experimental integrity due to being identical and not influenced by outside factors, were removed from observation. After each group of cells reached a count exceeding 5 million, a western blot was performed to confirm full knockout of NT5C2 and observation of growth and behavior continued.

Rescue of NT5C2 KO cells

Similarly to initial procedures for the CRISPR knockout, rescue gRNAs for NT5C2 were designed using BenchLink and the full gRNA-GFP-puroresistance complex plasmids were obtained from a supplier and transformed into *E. coli* bacteria. After selection for successfully transformed bacteria with puromycin, plasmids with extracted with the QuiaGen DNeasy

Extraction kit following standard protocol. Bacterial minipreps performed with Zymo Miniprep Kit, according to standard procedure. The rescue gRNAs were transformed into 293T packaging cells and, after an incubation period, the cells were lysed and the plasmids were lentivirally infected into 10cm plate of T-ALL cells, leaving one negative control of a plate not infected with gRNA. After induction of Cas9, confirmation of successful rescue was performed using western blotting and growth curve assays were used to identify any effect of the rescue compared to WT, KO, and mutant variants.

Identification of compensatory mechanisms

Extraction of RNA of generated NT5C2 KO, WT, and mutated ALL cells was performed using the QuiaGen RNA extraction kit and standard protocol. RNA sequencing on these samples was performed in order to compare gene expression of each variant. Validation experiments with any genes of interest using shRNA knockdown of said genes in cells via MTT and malachite green assays were also initially planned.

Whole-genome CRISPR Screening

Whole-genome CRISPR screening was performed in order to identify genes conferring resistance or sensitivity to mizoribine. A whole-genome GeCKO gRNA pooled library, purchased from a supplier, was transfected into lentiviral vectors. The transfection was performed through the addition of 3 ug of the plasmid of interest, 2.7 ug GagPol combined lentiviral packaging plasmid, .3ug VSV-G lentiviral envelope plasmid, 18uL jetPEI transfection reagent, and 250 uL NaCl to wells as well as jetPEI transfection reagent suspended in an additional 250 uL NaCl prior to adding it to the DNA solution. After agitation and incubation, each of the solutions (one for every vector) was added onto an individual well of 293T cells. Following incubation, the 293T cells were lysed, leaving only the viral supernatant, with which infection of human T-ALL cells was performed with the plasmids with the produced lentiviral vector; specifically, using 24-well plates with 1 million cells per well for a final 1:1 cell:virus ratio by volume. After puromycin selection, cells were pooled into a flask (along with a concurrent, identially-sized CRISPR-free negative control pool). Samples were taken from each

group, followed by addition of 50 micromolar mizoribine. Additional representative samples were taken at Day 7 and Day 14 (the final day of the screening). Extraction of RNA from all time points was performed using QuiaGen RNA Extraction Kit according to standard procedure, and said samples underwent MaGeCK flute analysis to identify which genes were associated with increased resistance to mizoribine, as potential therapeutic targets. Validation experiments were performed for the top 5 identified genes of interest using shRNA knockdown of said genes in cells, followed by comparing their response to HTP-2, mizoribine, and 6MP in MTT assays. The whole-genome screening was afterwards identically performed with HTP-2 in place of mizoribine.

RESULTS

Mizoribine Screen Identifies Several Candidates

The HTP-2 screen as well as the RNA sequencing of NT5C2 variants failed to return usable results. However, multiple genes were identified as being associated with increased mizoribine sensitivity when absent after whole-genome screening. Genes conferring resistance when absent were also identified, though with less significance.

1 HDHD1	1 NT5C2
2 LMO2	2 HEATR3
3 AMPD2	3 TP53
4 LYL1	4 ADK
5 CREBBP	5 HNRNPM
6 UBE2H	6 CSNK2B
7 DEPDC5	7 MFN2
8 MARCH5	8 IARS2
9 ZNF248	9 GNL2
10 IMPDH2	10 ADSS
11 SPINK14	11 MRPL3
12 ENPEP	12 MLST8
13 PEF1	13 WTAP
14 ZAK	14 KAT5
15 NELFA	15 DLD

Figure 1. Left, top 25 genes associated with mizoribine sensitivity. Right, top 25 genes associated with mizoribine resistance. Strength of coloration is proportional to strength of sensitivity/resistance as determined by MaGeCK Flute analysis of RNAseq data for Day 0, treated, and control populations, statistically implementing copy number correction, batch effect removal, and normalization.

Validation of mizoribine screen

Validation of the top results of the mizoribine screen returned either marginally significant or insignificant results. There were no strong correlations between inhibition of the genes tested and either NT5C2 expression or mutant NT5C2 cell viability.

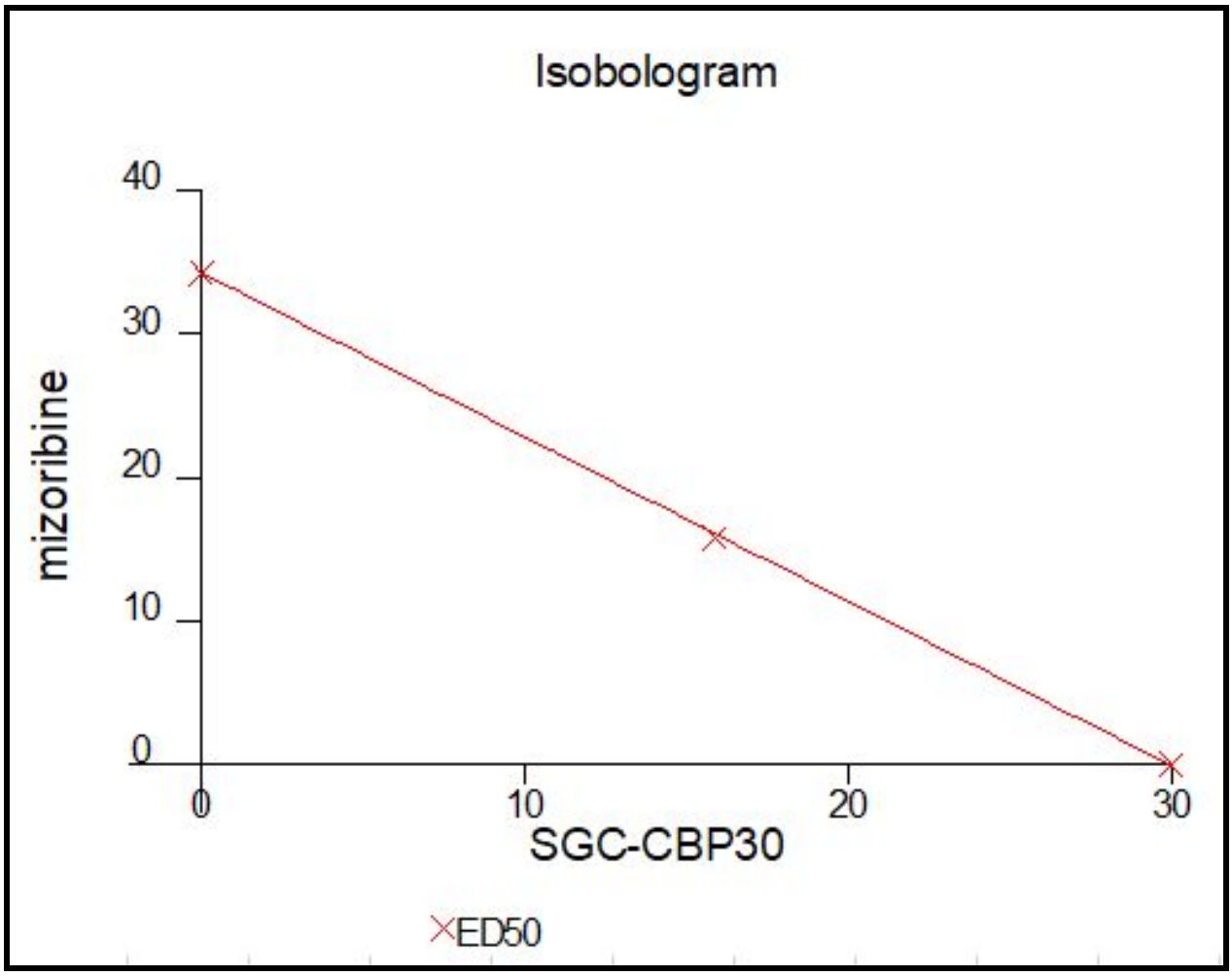

Figure 2. Isobologram analysis of MTT assay with mizoribine and SGC-CBP30. There is a marginal level of significance that SGC-CBP30 (CREBBP inhibitor) disproportionately amplifies the cytotoxic effect of mizoribine on NT5C2 mutant cells.

Variant growth

There was no significant difference between the growth or growth rate of NT5C2 KO, WT, or rescue CUTLL1 cells.

DISCUSSION

Knockout of NT5C2 does not affect growth or homeostasis of the ALL cell. While this means that NT5C2 inhibition alone cannot be counted on as a standalone ALL therapeutic, its potential to be used in conjunction with 6MP to eliminate chemoresistance is unaffected. This also indicates potentially decreased side effects if NT5C2 is used as a therapeutic in humans. NT5C2 is also clearly not an essential gene, which leaves open possibilities of using NT5C2 inhibition further

NT5C2 being the gene most strongly associated with mizorbine resistance when absent points to its primary function being in the purine biosynthesis pathway, as inhibition of a major component of that pathway (IMPDH) that has no other known or suspected functions is the only known function of mizoribine. This result also validates the basis of the genetic screen. However, the strong correlation of HDHD1 with mizoribine sensitivity when absent, a protein whose biological function is as of yet unknown, points to at least a secondary function for NT5C2. HDHD1 encodes a pseudouridine-5'-phosphatase, and as pseudouridine-5’-phosphate is primarily an intermediary in RNA degradation there is no evident correlation between potential HDHD1 functions and the purine biosynthesis pathway.

CREBBP is a large protein responsible for activating transcription and interacting with multiple transcription factors. While it has been associated with acute myeloid leukemia, a disease causally and symptomatically similar to ALL, this association has been centered on its oncogenesis via disruption of the cell cycle through aberrant transcription activation - unrelated to NT5C2’s aberrant role as conferring chemoresistance, or to the purine biosynthesis pathway. LYL1, like CREBBP, is involved in transcription, but as a transcription factor in B cells that is explicitly associated with ALL. LMO2 is also crucial to B cell differentiation. It is likely that the effect of these transcription-involved proteins was amplified by performing the screen in cancerous cells.

Interestingly, AMPD2 is involved in the purine biosynthesis pathway (contributing to said synthesis) but has also previously been associated with spastic paraplegia when rendered inactive by frameshift or nonsense mutations. As AMPD2 contributes to purine synthesis and may cause spastic paraplegia when deleted, while NT5C2 removes excess purines and may cause spastic paraplegia when aberrantly active, it may be that spastic paraplegia is in part caused by insufficient purine availability in the cell.

For future research, whole-genome screening with direct NT5C2 inhibitors, when available (or preliminary) should be performed. Additional, CRISPR KO testing of the identified genes' affect on ALL mutant cell viability should be performed.

WORKS CITED

Bahojwani, D., Yang, J. J., & Pui, C. H. (2015). Biology of childhood acute lymphoblastic leukemia. *Pediatric Clinics,* 62(1), 47-60.

Belver, Laura, and Adolfo Ferrando. "The genetics and mechanisms of T cell acute lymphoblastic leukaemia." *Nature Reviews Cancer* 16.8 (2016): 494.

Bhatia, S., Landier, W., Hageman, L., Kim, H., Chen, Y., Crews, K. R., & Maloney, K. W. (2014). 6MP adherence in a multiracial cohort of children with acute lymphoblastic leukemia: a Children's Oncology Group study. *Blood*, *124*(15), 2345-2353.

Chu, Q., Rathore, A., Diedrich, J. K., Donaldson, C. J., Yates III, J. R., & Saghatelian, A. (2017). Identification of Microprotein–Protein Interactions via APEX Tagging. *Biochemistry*, *56*(26), 3299-3306.

Dephoure, N., Zhou, C., Villén, J., Beausoleil, S. A., Bakalarski, C. E., Elledge, S. J., & Gygi, S. P. (2008). A quantitative atlas of Mitotic phosphorylation. *Proceedings of the National Academy of Sciences*, *105*(31), 10762-10767.

Dieck, C. (2018a). [High-throughput screening of various compound libraries for NT5C2 inhibitor]. Unpublished raw data.

Dieck, C. L., Tzoneva, G., Forouhar, F., Carpenter, Z., Ambesi-Impiombato, A., Sánchez-Martín, M., & Ferrando, A. A. (2018b). "Structure and Mechanisms of NT5C2 Mutations Driving Thiopurine Resistance in Relapsed Lymphoblastic Leukemia." *Cancer cell, 34*(1), 136-147.

Horiuchi, D., Collins, C. A., Bhat, P., Barkus, R. V., DiAntonio, A., & Saxton, W. M. (2007). Control of a kinesin-cargo linkage mechanism by JNK pathway kinases. *Current Biology*, *17*(15), 1313-1317.

Hunger, P.; Mullighan, G. (2015-10-14). "Acute Lymphoblastic Leukemia in Children". *New England Journal of Medicine. 373*(16): 1541–1552. doi:10.1056/nejmra1400972. PMID 26465987.

Kim, D. I., Jensen, S. C., Noble, K. A., KC, B., Roux, K. H., Motamedchaboki, K., & Roux, K. J. (2016). An improved smaller biotin ligase for BioID proximity labeling. *Molecular biology of the cell*, *27*(8), 1188-1196.

Tzoneva, G., Perez-Garcia, A., Carpenter, Z., Khiabanian, H., Tosello, V., Allegretta, M., ... & Paganin, M. (2013). Activating mutations in the NT5C2 nucleotidase gene drive chemotherapy resistance in relapsed ALL. *Nature medicine,* 19(3),368.

Tzoneva, G., Dieck, C. L., Oshima, K., Ambesi-Impiombato, A., Sánchez-Martín, M., Madubata, C. J., & Sulis, M. L. (2018). Clonal evolution mechanisms in NT5C2 mutant-relapsed acute lymphoblastic leukaemia. *Nature*, *553*(7689), 511.

Elsaid, M. F., Ibrahim, K., Chalhoub, N., Elsotouhy, A., Mudehki, N. E., & Aleem, A. A. (2017). NT5C2 novel splicing variant expands the phenotypic spectrum of Spastic Paraplegia (SPG45): case report of a new member of thin corpus callosum SPG-Subgroup. *BMC Medical Genetics,* 18(1). doi: 10.1186/s12881-017-0395-6